Lowland Technology International 2020; 22 (1):172 – 179
International Association of Lowland Technology (IALT): ISSN 1344-9656
Special Issue on: Engineering Geology and Geotechniques for Developing Countries

Research Paper

Slope Instability Evaluation Using Geophysical Methods of Gua Musang-Cameron Highland Highway

M.T. Zakaria [1], N.M. Muztaza [2*], H. Zabidi [3], F. Ahmad [4], T.O. Adeeko[5], N. Ismail [6] and N. Samsudin [7]

ARTICLE INFORMATION

Article history:

Received: 03 January, 2020
Received in revised form: 21 March, 2020
Accepted: 03 April, 2020
Publish on: 06 June, 2020

Keywords:

2-D Resistivity
Slope failure
Geophysics

ABSTRACT

Slope failure is a complex phenomenon that may trigger the occurrence of slope failure due to several factors. The internal structures and mechanical properties of subsurface are important parameters to investigate as a pre-requisite analysis. Four parallel survey lines of 2-D resistivity and two lines of seismic refraction were designed in order to achieve the objectives. The model shows the resistivity values covered of 1-4000 Ωm with investigation depth of 20 m. Highly weathered zones were identified at values of 400-450 Ωm while saturated zones with values of <100 Ωm. The high resistivity regions with values of 1500-2500 Ωm indicates the weathered granite for this area. The 2-D seismic refraction model shows velocity values ranging between 200-2800 m/s and depth coverage about 30 m. The result interpreted as 3 layer cases with 1st layer, 2nd layer, and 3rd layer identified at velocity of 400-600 m/s, 800-1400 m/s and >2000 m/s respectively. The low resistivity and velocity indicate as highly fractured/crack zones which able to decreases the shear strength of the slope soils and increases the hydraulic conductivity of the soils. The saturated zone and infiltration with the existence of boulders indicates the factor for the occurrence of slope failure.

1. Introduction

Slope failure is a complex phenomenon that may trigger the occurrence of soil creep and landslides due to several factors and become one of the major geomorphic processes that affected evolution landscape of the mountainous region and caused the disastrous phenomenon. The failure often occurs due to heavy rainfall following a long-lasting creeping caused by weakening of shear zones (Germer & Braun, 2011). The internal structures and mechanical properties of soil and rock mass of the slope are important parameters to investigate or estimated with a reasonable degree of certainty as a pre-requisite analysis. There are numerous landslide tragedies in Malaysia recorded and involves huge number of fatalities and economic loses. The slope failure event occurred mostly triggered by heavy rainfall due to tropical rainforest climate with relatively high temperature and receives rainfall throughout the year. Malaysia experience the hot and humid climate all year round with temperature 22-32 degree Celsius with annual rainfall from 200–250 cm and extremities during southwest (April-October) and northeast (October-February) monsoons (Yusoff et al., 2016). The combination of climatic parameters caused intense chemical weathering and formation of residual soil. Under

[1] Student, School of Physics, Universiti Sains Malaysia, Main Campus, Penang, Malaysia, taqiuddinzakaria92@gmail.com
[2*] Lecturer and Corresponding author, School of Physics, Universiti Sains Malaysia, Main Campus, Penang, Malaysia, mmnordiana@gmail.com
Note: Discussion on this paper is open until December 2020

certain geological and topography effect, the rainfall become major factor triggered the occurrence of landslides involving both natural and cut slopes. The situation become more critical in highland area which often receive more precipitation. The hilly area stables within a certain range of water saturation, under the critical limit the shear resistance of soil is enhanced due to effect of suction which creates an apparent cohesion between particle (Springman et al., 2003). Major landslides at local slope failure occurs due to water saturation exceeds a critical limit in certain parts of the slope (Friedel et al., 2006). The infiltration of rainfall into soil and its effect on slope failure has been of particular interest for the past few years (Irfan et al., 2017; Chen et al., 2018,2019; Jing et al., 2019). Rahardjo et al. (2015) conducted a series of parametric studies to understand the hydrological and geotechnical parameter on its rainfall-induced instability. The result shows the rainfall intensity, soil properties, ground water table, and slope geometry plays an important role in rain—induced instability of the slope. The continuous infiltration of rainwater will increase the pore-air pressure and decreases the matric suction which compromising the slope stability (Sun et al., 2015, 2016). The process causes change in effective stress which produced the variations in porosity (Sun et al., 2016). According to Collins and Znidarcic (2004), two distinct failure mechanism have been observed for rainfall-induced landslides. For the first mechanism, significant build-up of positive pressures is observed in a low area on the slope or along the soil/bedrock interface. Movements along the sliding surface lead to liquefaction along it, resulting in rapid movements, long run-out distances and finally a complete liquefaction of the failed mass (Wang and Sassa, 2001). In the second mechanism, the soil in the unsaturated state, and slope failure is due mainly to rainfall infiltration and a loss in shear strength when soil suctions are decreased or dissipated (Fourie et al., 1999). Infiltration and near-surface flow create an increase in pore water pressure that causes the stress path to move nearly horizontally to intersect a failure envelope, initiating a slope failure. In unsaturated loose soils, suction decrease and coupled volumetric collapse may be involved in the failure process (Olivares and Picarelli, 2003). Landslides in weathered granitic rocks are strongly affected by types of weathering and have been documented in tropical and humid regions. Based on a study conducted by Chigira et al. (2011) granitic rock are known to be very sensitive to weathering and vulnerable for mass sliding. In wet tropical region in Malaysia, deep weathering profile will exhibit a thickness up to 100 m. The mechanism of failure is highly controlled by the nature of weathered material and its mass structure. Typical weathering profile of granite consist of decomposed granite with core stones in the lower part and saprolite in the upper part. The rock loosed rapidly as it was exposed to the ground surface and formed a loosed layer to slide. Dynamics of weathered material under saturated conditions, high erodibility, existence of relict discontinuities, sharp soil-rock boundary and the inhomogeneity of weathering structures will lead to frequent slope failure events. Fracture and any structural discontinuity reduce cohesion and internal friction by severing bonds between particles and creating discrete failure surfaces (Terzaghi, 1962; Carson and Kirkby, 1972). In general, rock mass strength decreases over increasing spatial scales as the fractured and discontinuities increased. Intersecting fractures have potential to completely disintegrate rock fragments, which turn minimizes cohesion at decimetre to meter scale resulted in reducing internal friction to the friction between disjointed fragments, as opposed to the friction between mineral grain within the intact rock. Hence, developing a scientific comprehension of the geological and physical process of earth's rheology are important to evaluate and to conduct a predictive model for hazard problems. Therefore, 2-D resistivity and seismic refraction survey was utilized to visualizes the failure zones as purpose to identify the subsurface characteristics with the trigged factors for the slope failure for this study. The geophysical methods have been successfully applied in this study as a non-destructive method and environmentally friendly in order to provide an exhaustive subsurface image resolution with less time consumption and cost. Four survey lines of 2-D resistivity and two seismic refractions was conducted at hill cut slopes along the Gua Musang-Cameron Highland Highway.

2. Methodology

2.1 Study area and geological setting

The study area located along the highway of Gua Musang-Cameron Highland which is part of the Main Range. The 2-D resistivity and seismic refraction survey was designed at the terrace of the cut slope as shown in Figure 1. From the field observation the surface condition was severely disturbed as the creeping activity seismically active where some part of the soil already fall (Figure 2). The creeping activity occurs at estimated dimensions of length of (20 m) x width (30m) from the surface

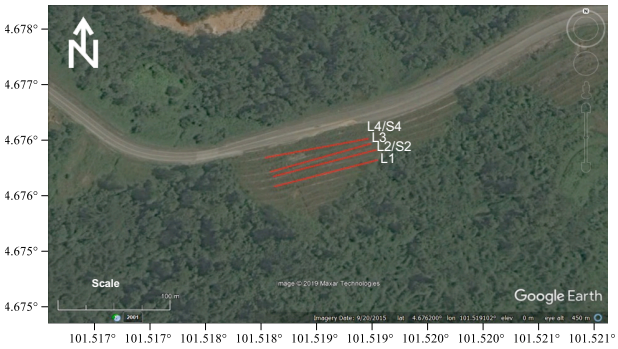

Fig. 1. Study area.

Fig. 2. Images of study area

This Main Range consists mostly of granite with several enclaves of metasedimentary rocks (Raj, 2009). The Main Range Granite is located in west of the state stretching along western Kelantan up to the state boundary of Perak and Pahang, and also the international boundary of Malaysia -Thiland. Reported by Rahman and Mohamed in 2001, the distribution of igneous rock in Kelantan is in the west and east part of borders state which is the Main Range Granite and Boundary Range Granite. The Main Range Granite is generally of a Late Triassic age. Figure 3 show the general geology of the area where most of the parts categorized as acid intrusive which commonly refer as granite.

Figure 4 shows the 3-D topography of the study area where the lowest elevation was recorded at 490 m from sea level whereas the highest part at 670 m. The high topography landscape was dominant for this area as it shows the most potential area for slope instability to occurred. Majority of the land here was used for farm plantation as this area are famous for agriculture-based economy. There are many farm plantation was setup at the slope topography which may lead the instability of ground condition.

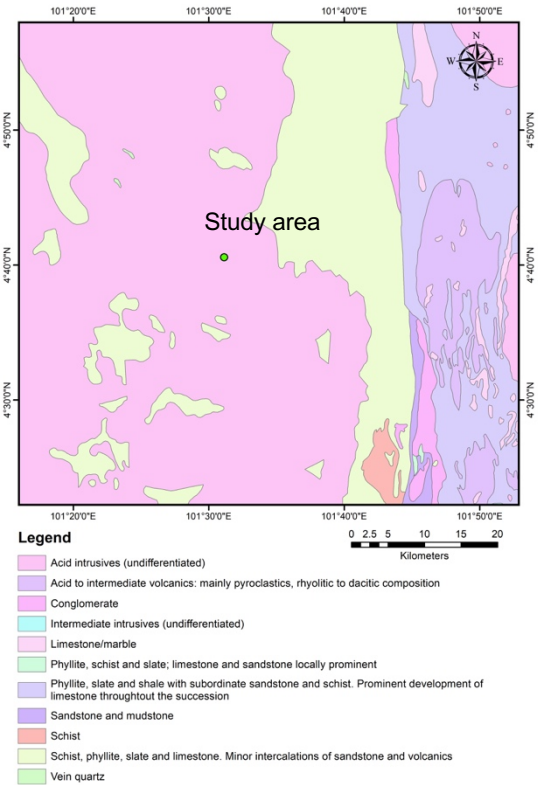

Fig. 3. Geological map of study area.

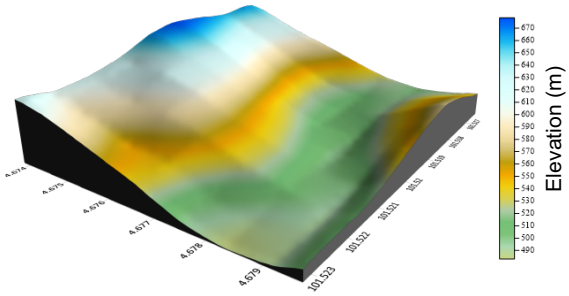

Fig. 4. 3-D topography of study area.

2.1 Field procedure of 2-D resistivity

2-D resistivity consists of experimental determination of apparent resistivity of given material, through joint measurement of electric current intensity and voltage injected into subsoil through separate couples of electrodes throughout the ground surface. The 2-D resistivity is measured using 41 electrodes in linear array with investigated depth of one fifth of survey length and connected to multichannel cables. The resistivity distribution can be interpreted in terms of soil lithology and saturation. ABEM SAS4000 system with Wenner-Schlumberger array were used to acquire the data which provide good signal resolutions of vertical and horizontal. The 2.5 m minimum electrode spacing were used based on the site constraint and depth of interests not more than 30 m. Four parallel survey lines were designed in such way to fulfil the objective of the study with length of

100 m. The resistivity data was processed in Res2Dinv software for inversion model and Surfer8 software for interpretation and correlation. The processed and filtered data are inverted using the least square inverse technique with smoothness constraint and Gauss-Newton optimization technique (Loke, 1997a; Loke, 1997b). The calculated apparent resistivity values of the model block are compared with measured apparent resistivity values. It is adjusted iteratively until the values of the model have closed an agreement with measured apparent resistivity values. The results obtained were presented in 2-D resistivity inversion model where the range of resistivity values were indicated by a color scale.

2.2 Field procedure of seismic refraction

Seismic refraction tomography is based on the determination of time interval that elapses between initiation of seismic waves at a certain shot point and the arrival of refracted waves at one or more seismic detector. Seismic waves propagate different velocity when traveling in different types of geological layer and refracted when they encounter geological boundary governed by Snell's Law. In a seismic refraction survey, two survey line were designed in line with resistivity lines of L2 and L4. The seismic lines labelled as S2 and S4 were acquire using ABEM Terraloc MK8 system with 28 Hz geophone spacing of 5 m. Seven shot points were used which are five inline and two for offset to produce comprehensive data resolutions. Seismic data were processed using FirstPix software for picking first arrival time, plotting travel time curve, and velocity analysis. The output was used in SeisOpt2D for generated the 2-D seismic profiles. The seismic refraction result is displayed in Surfer8 software for interpretation and correlation. The result obtained is presented in 2-D profiles with a different color scale representing different velocity values.

3. Result and Discussion

The result (Figure 5) shows the 2-D inversion model of resistivity of L1-L4 with resistivity values ranging between 1-4000 Ωm and investigation depth of 20 m. The analysis of this model reveals the characteristic for the profile as highly weathered zones were identified at values of 200-450 Ωm while saturated zones with values of <100 Ωm. The high resistivity region for all profiles with values of 1500-2500 Ωm indicates the weathered granite at this area. The contrast of the resistivity regions (low-high-low) or (high-low-high) indicated the existence of fracture zones (black dashes line) for this area at resistivity values ranging from 250-550 Ωm. Resistivity values of >2000 Ωm represent the boulders for this area with a depth of 3-10 m from the ground surface.

The low resistivity region which indicated as highly saturated zones contribute as the factor of the occurrence mass movement of the soil profile dominated by the sand and sandy silt. The continuous infiltration of surface water and heavy rain as it is seeping through to fracture area and accumulated may trigger the instability of the slope as the permeability and the porosity of the soil is higher. The disturbance of the soil properties with the variation of porosity and permeability increased the effectives stress of the soil which able to trigger the mass movement for the instability slope. Soils often exhibit a variety of heterogeneities, such as fractures, cracks, macro-pores of biotic origin, and inter-aggregate pores (Novak et al., 2000; Zhang and Li, 2010). Preferential flow due to anisotropy of hydraulic conductivity or due to flow through relic joints may be present in natural soils (Zhang et al., 2000). For slopes that are initially unsaturated, the effect of rainfall at the slope surface will have a different effect. The pore water pressure pattern that develops in the soil will occur as a transient process as the infiltrating water moves downwards into the soil. In unsaturated loose soils, suction decrease and coupled volumetric collapse may be involved in the failure process (Olivares and Picarelli, 2003). Localised transient pore water pressures due to particular hydraulic boundary conditions may also be a triggering mechanism for the transition from slide to flow. The hillslope soil condition generalized as partially saturated with sandy and silty soil dominant for all profiles which possible the occurrence of slope failure under the continuous infiltration of the surface water and rain fall.

The occurrence of the fracture zones/crack provided a wider zone for surface water to seep through to the soil and accumulated. The unstable condition with loose materials and increased accumulation of water triggered the occurrence of slope failure. The failure zone was identified for this area as the existence of the fracture zone/crack with the boulder that may trigger the occurrence of the mass movement. The presence of cracks in a slope decreases the shear strength of the slope soils and increases the hydraulic conductivity of the soils. Water-filled cracks also lead to additional driving forces. In addition, the cracks may form part of the slip surface when landslide occurs. The presence of the boulder can be a key factor for the instability due to change and removing the rock that holds the slope in place (Nelson, 2013: Filip et al., 2017). The existence of low resistivity zones within granite body indicate as highly fractured and water conducting zones. The residual soil layers are relatively thin at zones where granite dominates the slope face of the failure mass. This study shows the water flow/saturated zone were identifying as weak zone or a plane of weakness.

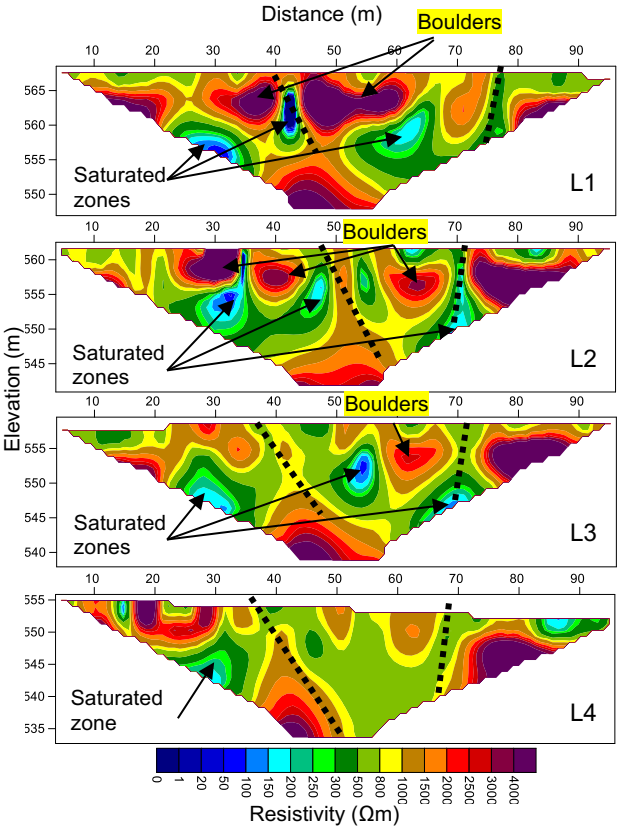

Fig. 5. 2-D inversion model of resistivity of L1-L4

High resistivity values at depth <5 m for lines, L1 and L2 indicate the presence of boulder for this area. The hard layer/ bedrock identified at resistivity values >3000 Ωm for all line profiles with of depth 10-15 m. The result shows the flow pattern of isolated low resistivity zones from L1-L4 (black arrow) at distance of 20-30 m and 55-65 m with depth of 5-10 m. Rainfall seasons in tropical region is also one of the factors that need to be consider. Heavy and continuous precipitation may lead instability of the slope as the soil become fully/nearly saturated to mobilize into debris flow. The highly weathered and loose particle may trigger the instability condition. Figure 6 shows the 3-D orientation of the results of survey lines according to the field – scale observation with the creep zone highlight with light reddish color, indicated the current condition of the creep/slope failure event. The boundary of creep zone boundary was shown with dash-black lines.

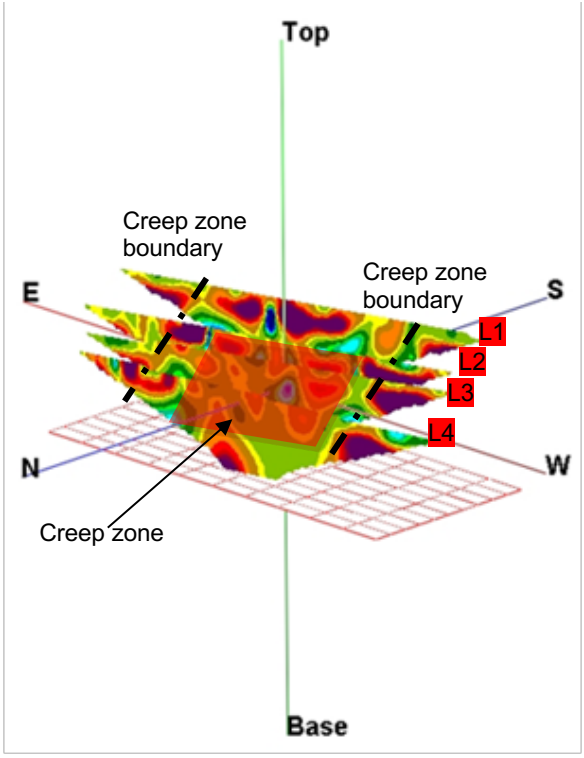

Fig. 6. 3-D orientation of inversion model of resistivity of L1-L4 with creep zone of the field-scale observation

Figure 7 shows the 2-D seismic refraction model of S2 and S4 with velocity values ranging between 400-2800 m/s and depth coverage about 30 m. The result interpreted as three main layers of velocity representing three types of geo-materials with possible different characteristics. The first layer identified at velocity ranging between 400-600 m/s with depth of <5 m from the surface. The velocity increased as the depth of penetration increased up to 20 m with velocity of 800-1400 m/s for second layer. At depth of >20 m with velocity of >2000 m/s considered as 3rd layer cases for the profiles. In this study, the velocity profiles show heterogeneous subsurface models of the creep zones for this area. The velocity of 400-600 m/s represent the loose soil of the materials while velocity of 800-1400 m/s represent the highly weathered materials. The trends continuous for S2 and S4 with hard material/bedrock identified at depth >20 m with velocity of >2000 m/s which considered moderately weathered granite. The variation of weak zones obtained from the result may occurs because of the present subsurface materials undergo additional weathering process thus producing another poor rock mass quality. The extremely weather climate leads the progressive weathering processes due to abundance of rainfall and moisture as accelerating the transformations of homogenous subsurface material in heterogeneous condition (Abidin et al., 2012a). Major

new fractures may form or be extended as the incipient fractures may lose tensile strength and the discontinuity of rock wall become weak, which later reduce the shear strength and stiffness (Dearman et al., 1995). In addition, the earthwork history involving cut and fill materials on the original topography may also weaken the ground foundation for long-term process since the water flow, soil and rock condition was already disturbed and altered (Abidin et al., 2012b).

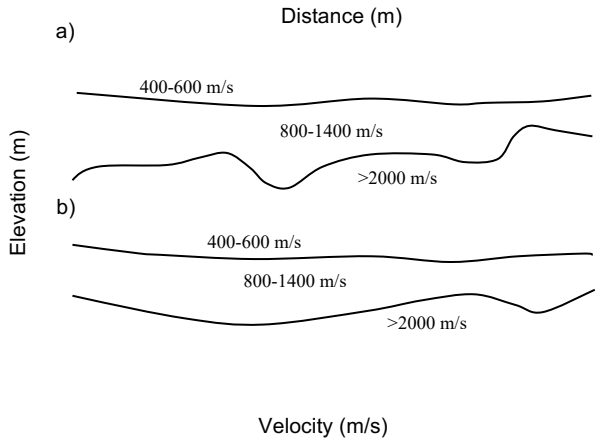

Fig.7. 2-D seismic refraction profile; a) S2; b) S4.

4.2 Density estimation from 2-D seismic refraction

Density is an important parameter to differentiate the lithology and estimate the other petro-physical parameters such as porosity, or fluid content. Many geological interpretations involve the conventional relationship between density and velocity. Density commonly estimated from seismic velocity using a set of relationship such as Birch (1961), Gardner et al. (1974) and Lindseth (1979). Gardner's relation subsequently correlated in the variation of bulk density from wide range of basins, ages, depths from which a density-velocity relationship was develop as shown below.

$$\rho = 0.31V_p^{0.25} \quad (1)$$

where ρ is bulk density given in g/cm^3, and V_p = P-wave velocity (m/s).

Figure 8 shows the interpolated result (dashed box) of density model using 2-D seismic refraction. The results were correlated with 2-D resistivity as saturated zones correspond with low bulk density distributions of 1.2-1.8 g/cm^3. The estimated density models show directly proportional with depth. From figure 8 it shows that low resistivity (<100 Ωm) potentially for triggering the soil the slope instability as it become fully/nearly saturated. The infiltration of rainwater into the unsaturated soil decreases the matric suction, hence affecting the shear strength properties and thus the probability of slope failure. This condition will further decrease the shear strength of soil and eventually make the slope increasingly susceptible to failure (Gofar and Rahardjo, 2017). The infiltration of rainwater increases the bulk density of the soil as the permeability also increases making the soil gradually saturated in the initial stage (Jing et al., 2019). The continuous process of the infiltration with heavy precipitation will leads the instability of the slope. The estimated density model for L2 and L4 shows the bulk density is gradually increasing as the depth increase. This may indicate that the subsurface was partially saturated as the resistivity shows low values of <100 Ωm.

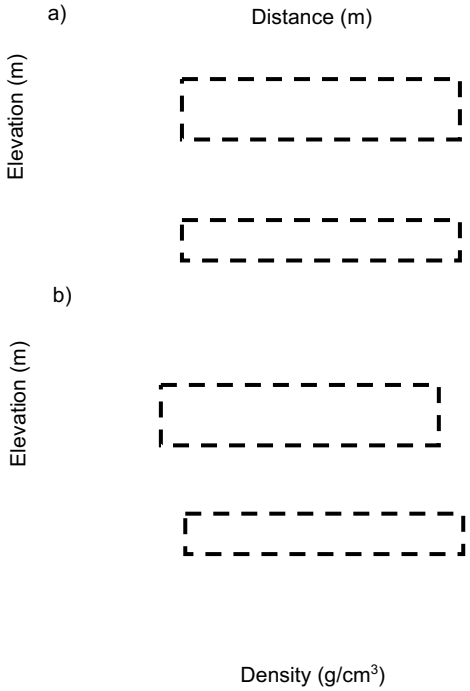

Fig. 8. 2-D resistivity and estimated density model from seismic refraction: a) L2; b) L4

4. Conclusion

The geophysical method successfully applied in investigation subsurface characteristic for slope failure. The result from 2-D resistivity and seismic refraction shows the hillslope soil condition generalized as partially saturated consist of sand, sandy silt and loos materials that dominant for all profiles which possible the occurrence of slope failure under the continuous infiltration of the surface water above the water table. The presence of boulder or additional mass represents the additional factor for the slope failure. The existence of fracture/crack zones increased the accumulation of the water as the continuous infiltration will reduced the shear strength of the slope soils and increases the hydraulic

conductivity of the soils which lead to the slope failure. The study shows that geophysical method was useful in delineating the subsurface characteristic besides the information was useful for rehabilitation and mitigation purposes. This geophysical method is suitable for our sustainable ground investigation since it can reduce time, money and provided comprehensive subsurface data interpretations. Table 1 and 2 shows the summary of the result of 2-D resistivity and seismic refraction.

Table 1. Summary of the 2-D resistivity result

Factor of Slope Failure	Descriptions
Fracture zone/crack	200-550Ωm, the occurrence of the fracture zones provided a wider zone for surface water to seep through to the soil and accumulated. The changes of soil condition and properties with the variation of porosity and permeability increased the stress of the soil which able to trigger the slope failure.
Saturated zone	<100Ωm, Heavy and continuous precipitation may lead instability of the slope as the soil become fully/nearly saturated to mobilize into debris flow
Boulder	>2000Ωm the presence of the boulder can be a key factor for the instability due to change and removing the rock that holds the slope in place
Precipitation	Heavy rain and continuous rain change the soil condition become fully/nearly saturated to trigger the instability

Table 2. Summary of seismic refraction

Velocity layers	Descriptions
First layer	Velocity ranging between 400-600 m/s with depth of <5 m from the surface
Second layer	The velocity increased as the penetration increased up to 20 m with velocity of for 2nd layer case. Velocity ranging 800-1400 m/s which consider as highly weathered zones
Third layer (bedrock)	Hard material/bedrock identified at depth >20 m with velocity of >2000 m/s which considered moderately weathered granite

Acknowledgements

The author wishes to thank, all lecturers, staffs, and postgraduate student from geophysics section Universiti Sains Malaysia (USM) for their assistance during the geophysical data acquisition. The author wishes to thank USM for providing the Research University Grant (RUI) entitled of Geophysical Application and Approaches in Engineering and Environmental Problems (1001/PFIZIK/811323) and Fundamental Research Grant Scheme (FRGS) entitled of Development of 2-D Linear Inversion Algorithm from Geophysical Approach for Soil or Rock Characteristics for research funding (203/PFIZIK/6711663). Special thank also to USM Fellowship for providing the tuition funding.

References

Abidin, Z., Hazreek, M., Saad, R., Ahmad, F., Wijeyesekera, D.C., Baharuddin, T. and Faizal, M., 2012b. Seismic refraction investigation on near surface landslides at the Kundasang area in Sabah, Malaysia. *Procedia Engineering*, **50**: 516-531.

Abidin, Z., Hazreek, M., Saad, R., Fauziah, A., Wijeyesekera, C., Baharuddin, T. and Faizal, M., 2012a. Integral analysis of geoelectrical (resistivity) and geotechnical (SPT) data in slope stability assessment. *Academic Journal of Science*, **1** (2): 305-316.

Birch, F., 1960. The velocity of compressional waves in rocks to 10 kilobars, Journal of Geophysical Research, **65** (4):1083-1102.

Carson, M. A., and M. J. Kirkby, 1972. Hillslope Form and Process, Cambridge Univ. Press, London.

Chen, Y., Irfan, M., Uchimura, T., Wu, Y. and Yu, F., 2019. Development of elastic wave velocity threshold for rainfall-induced landslide prediction and early warning. Landslides, **16** (5): 955-968.

Chen, Y.L., Irfan, M., Uchimura, T., Nie, W. and Cheng, G.W., 2018. Elastic wave velocity monitoring as an emerging technique for rainfall-induced landslide prediction. Landslides, **15**: 1155–1172.

Chigira, M., Mohamad, Z., Sian, L. C. and Komoo, I, 2011. Landslides in weathered granitic rocks in Japan and Malaysia. Bulletin of the Geological Society of Malaysia, **57**: 1-6.

Collins, B.D. and Znidarcic, D., 2004. Stability analyses of rainfall induced landslides. Journal of Geotechnical and Geoenvironmental Engineering, **130** (4): 362-372.

Filip, D., Kacper, J., Marek, K. and Piotr, M., 2017. The role of landslides in downslope transport of caprock-derived boulders in sedimentary tablelands Stołowe Mts, SW Poland. Geomorfology, **295**: 84–101

Fourie, A.B., Rowe, D. and Blight, G.E., 1999. The effect of inÆltration on the stability of the slopes of a dry ash dump. Geotechnique, **49** (1):1-13.

Friedel, S., Thielen. A. and Springman, S.M., 2006. Investigation of a slope endangered by rainfall-induced landslides using 3D resistivity tomography and geotechnical testing. Journal of Applied Geophysics, **60** (2):100-114.

Gardner, G.H.F., Gardner, L.W. and Gregory, A.R., 1974. Formation velocity and density—The diagnostic

basics for stratigraphic traps, Geophysics, **39** (6): 770-780.

Germer, K. and Braun, J., 2011. Effects of saturation on slope stability: laboratory experiments utilizing external load, Vadose Zone Journal, **10** (2): 477-486.

Gofar, N. and Rahardjo, H., 2017. Saturated and unsaturated stability analysis of slope subjected to rainfall infiltration. MATEC Web of Conferences, **101**: 05004.

Irfan, M., Uchimura, T. and Chen, Y., 2017. Effects of soil deformation and saturation on elastic wave velocities in relation to prediction of rain-induced landslides. Engineering Geology, **230**: 84-94.

Jing, X., Chen, Y., Pan, C., Yin, T., Wang, W. and Fan, X., 2019. Erosion failure of a soil slope by heavy rain: laboratory investigation and modified gas model of soil slope failure. International Journal of Environmental Research and Public Health, **16** (6): 1075.

Jing, X., Chen, Y., Pan, C., Yin, T., Wang, W. and Fan, X., 2019. Erosion Failure of a Soil Slope by Heavy Rain: Laboratory Investigation and Modified GA Model of Soil Slope Failure. International journal of environmental research and public health, 16 (6):1075.

Lindseth, R.O., 1979. Synthetic sonic logs - A process for stratigraphic interpretation, Geophysics, 44 (1): 3-26.

Loke, M. H., 1997a. Electrical imaging surveys for environmental and engineering studies. A practical guide to 2-D and 3-D surveys: 61.

Loke, M. H., 1997b. Software: RES2-DINV. 2-D interpretation for DC resistivity and IP for windows 95. Copyright by MH Loke 5, Cangkat Minden Lorong 6, Minden Heights, 11700 Penang, Malaysia.

Nelson, A., 2013. Slope Stability, triggering events, mass movement hazards. Nat.Disasters.

Novak, V., Šimåunek, J. and Genuchten, M.T.V., 2000. Infiltration of water into soil with cracks. Journal of Irrigation and Drainage Engineering, **126** (1): 41-47.

Olivares, L. and Picarelli, L., 2003. Shallow flowslides triggered by intense rainfalls on natural slopes covered by loose unsaturated pyroclastic soils. Géotechnique, **53** (2): 283-287.

Rahardjo, H., Ong, T.H., Rezaur, R.B. and Leong, E.C., 2007. Factors controlling instability of homogeneous soil slopes under rainfall. Journal of Geotechnical and Geoenvironmental Engineering, **133** (12): 1532-1543.

Rahman, C.A. and Mohamed, K.R., 2001. Pemetaan awalan sumber warisan geologi negeri kelantan. In: Ibrahim Komoo, Tjia, H.D., and Mohd Shafeea Leman (eds) Geological Heritage of Malaysia (Geoheritage Mapping and Geosite Characterization), LESTARI UMK, Bangi: 27-39.

Raj, J. K., 2009. Geomorphology. In: Hutchison, C.S. and Tan, D.N.K (eds) Geology of Peninsular Malaysia, Geological Society of Malaysia, Kuala Lumpur: 5-29.

Springman, S., Jommi, C., and Teysseire, P., 2003. Instabilities on moraine slopes induced by loss of suction: a case history. Geotechnique, **53** (1): 3–10.

Sun, D.M., Li, X.M., Feng, P. and Zang, Y.G., 2016. Stability analysis of unsaturated soil slope during rainfall infiltration using coupled liquid-gas-solid three-phase model. Water Science and Engineering, **9** (3): 183-194.

Sun, D.M., Zang, Y.G. and Semprich, S., 2015. Effects of airflow induced by rainfall infiltration on unsaturated soil slope stability. Transport in Porous Media, **107** (3), 821-841.

Terzaghi, K., 1962. Stability of steep slopes on hard unweathered rock, Géotechnique, **12** (4): 251–270.

Wang, G. and Sassa, K., 2001. Factors affecting rainfall-induced flowslides in laboratory flume tests. Geotechnique, **51** (7): 587-599.

Yusoff, Z.M., Azmi, N.A., Nahazanan, H., Daud, N.N.N. and Aziz, A.A., 2016. Engineering geological of an active slope in km46 simpang pulai, perak. Malaysian Journal of Civil Engineering, **28**.

Zhang, J., Jiao, J.J. and Yang, J., 2000. In situ rainfall infiltration studies at a hillside in Hubei Province, China. Engineering Geology, **57** (1-2): 31-38.

Zhang, L.M. and Li, X., 2010. Microporosity structure of coarse granular soils. Journal of Geotechnical and Geoenvironmental Engineering, **136** (10): 1425-1436.

Symbols and abbreviations

2-D	Two-dimensional	m	meter
Ωm	Ohm.meter	cm^3	cubic centimeter
<	less than	g	gram
>	greater than		